Published 2003 Wiley-Liss, Inc.† Cytometry Part A 52A:90–100 (2003)

Comparison of Reagents for Shape Analysis of Fixed Cells by Automated Fluorescence Microscopy

John T. Elliott, Alessandro Tona, and Anne L. Plant

Biomolecular Materials Group, Biotechnology Division, Chemical Science and Technology Laboratory, National Institute of Standards and Technology, Gaithersburg, Maryland

Received 6 February 2002; Revision Received 22 October 2002; Accepted 31 October 2002

Background: Cell size and shape have been implicated as potentiators of intracellular signaling events and as indicators of abnormal cell behavior. Automated microscopy and image analysis can provide quantitative information about the size and shape of cultured cells, but it requires that the edge of a cell be clearly identified. Generating adequate contrast at the edge of thin well-spread cells can be challenging.

Methods: We compared six (five chemically reactive and one lipophilic) fluorescent molecules—5-chloromethyl fluorescein diacetate (CMFDA, CellTracker green), fluorescein-5-maleimide, fluorescein-5-isothiocyanate (FITC), 5-iodoacetamidofluorescein, 5(6)-carboxy fluorescein-*N*-hydroxysuccinimidyl ester, and N-fluorescein-1,2-dihexadecanoyl-sn-glycerol-3-phosphoethanolamine—for their effectiveness as stains for automated morphology analysis of fixed cells.

Results: Formaldehyde-fixed rat aortic smooth muscle cells stained with fluorescein-5-maleimide or FITC exhibited an average intensity that was at least twofold greater than cells stained with CMFDA even when subjected to a 25-fold shorter exposure time. Cell area determined with the higher intensity stains was less sensitive to threshold settings during automated cell morphology analysis.

Conclusion: A procedure that includes the use of fluorescein-5-maleimide or FITC for staining fixed cell provides sensitivity sufficient to permit rapid, automated, morphologic analysis of well-spread fixed cells. Cytometry Part A 52A:90–100, 2003.
Published 2003 Wiley-Liss, Inc.†

Key terms: automated fluorescence microscopy; quantitative microscopy; cell morphology analysis; stain; fluorescent dyes

Optical microscopy with the use of a computer-controlled translation stage and a charge coupled device (CCD) camera provides the opportunity to capture and digitize images of large numbers of cells over many fields in an unbiased manner. Current image processing software adds the ability to rapidly quantitate many cellular properties (cell density, morphology, protein expression, enzymatic activity, etc.), thereby offering the opportunity to accurately and efficiently quantitate cell properties and their associated population distributions (1–3). Successful automation of image collection and analysis requires that the specific features of interest exhibit sufficient contrast with respect to the background, i.e., these features must exhibit a significantly higher intensity than the background intensity. Good contrast allows the use of a threshold value to distinguish pixels associated with the object from those attributed to the background. The threshold value defines the intensity value below which is considered background and above which defines the features of interest. To improve discrimination between the background and the features of interest, cells are often labeled with chromophore or fluorescent reagents to enhance the contrast between cells and non-cell areas.

Many biological stains have been developed that target various cellular components or organelles (4–8). The choice of stain depends on the application, and some applications are more demanding than others. Fluorescent labels are often ideal reagents because the background fluorescent levels are relatively low in biological samples and the available fluorophores can have high quantum yields (9). In addition, fluorescent reagents with various excitation and emission wavelengths are available,

Certain commercial products are identified to adequately specify the experimental procedure; this does not imply endorsement or recommendation by National Institute of Standards and Technology.

†This article is a US government work and, as such, is in the public domain in the United States of America.

According to ISO 31-8, the term "molecular weight" has been replaced by "relative molecular mass," m_r. The conventional notation, rather than the ISO notation, has been employed for this publication.

*Correspondence to: John T. Elliott, Biomolecular Materials Group, Biotechnology Division, Chemical Science and Technology Laboratory, National Institute of Standards and Technology, Gaithersburg, MD 20899.

E-mail: jelliott@nist.gov

Published online in Wiley InterScience (www.interscience.wiley.com).
DOI: 10.1002/cyto.a.10025

thereby allowing multiple fluorophores to be used simultaneously on the same sample (9,10).

There many examples of the use of automated microscopy. One of the most common uses is the detection of "rare events" within a population of cells (11–15). For example, embedded tissue samples or cellular suspensions can be mounted on a glass slide and labeled with fluorescent antibodies for specific antigens. Some reports have shown that automated methods can detect one rare event among a million cells due to the high rate of sampling and discrimination (13,16). In other applications, fluorescent nuclear stains such as 4,6-diamidino-2-phenylindole have been used with automated microscopy to determine cell density (11). Multicolor approaches allow the use of automated microscopy to quantitate a particular stain intensity in an area defined by another stain. For example, cell proliferation has been evaluated by quantifying the intensity of fluorescent anti-bromodeoxyuridine antibodies in the nucleus, the area of which is defined by the TO-PRO-3 nuclear stain (17). If the different fluorophores have sufficiently different spectral properties, their fluorescent signatures do not interfere with each other. Some non-fluorescent reagents become fluorescent when enzymatically processed within a cell (5,6). By using laser scanning cytometry (18), real-time imaging of enzymatic activity within living cells can be achieved (19–21). It is important to note that these automated microscopy techniques provide information about each object detected, thus providing a population distribution of a particular cellular property (19,22).

One cellular property that is useful to examine by automated microscopy is cell morphology. Cell shape has been implicated as a potentiator of downstream integrin-mediated signaling events (23,24) and as a regulator of apoptosis (25,26). In addition, abnormal cell shape can be diagnostic for cancerous cells (27). Although fully automated high-throughput cell shape analysis is used in hematology and pathology laboratories for screening tissue samples for the presence of abnormal cells (16,28,29), its use with cells in culture can be challenging. Successful automation of morphology analysis of well-spread cells in culture requires that the edge of the cell be clearly distinguishable from the background. One way to approach this is to use dyes that spread throughout the cell cytoplasm. Because dye intensity is proportional to concentration and pathlength in the cell, this approach works well when cells have sufficient volume near the edge of the cell (30). Identifying the edge of a thin, well-spread cell, where the effective pathlength is small, can be difficult.

We compared several fluorescent labeling reagents and some of the parameters involved in automated cell shape analysis. We examined a lipid fluorophore, *N*-fluorescein-1,2-dihexadecanoyl-sn-glycerol-3-phosphoethanolamine (fluorescein-DHPE); two amino reactive fluorophores, fluorescein-5-isothiocyanate (FITC) and 5(6)-carboxy fluorescein-N-hydroxysuccinimidyl ester (F-NHS); and three fluorescent conjugating reagents that target sulfhydryl groups, 5-iodoacetamidofluorescein (5-IAF), fluorescein-5-maleimide, and 5-chloromethyl fluorescein diacetate (CMFDA). The fluorescein-5-maleimide and FITC dyes showed the best contrast at the edge of fixed cells. These two reagents allowed short exposure times for rapid analysis and were highly efficient indicators of total cell area.

METHODS AND MATERIALS

Coverslip Preparation

Glass 1 coverslips (22 × 22 mm) were washed in 1% sodium dodecyl sulfide (SDS; Sigma, St. Louis, MO), rinsed extensively with nanopure H_2O (Millipore Corp., Bedford, MA), and acid washed in fresh H_2SO_4 containing 10% potassium persulfate (30 min). The coverslips were rinsed extensively with nanopure H_2O, transferred to acetone, and dried on a particle-free polyester wipe cloth (Texwipe TX1010, Fisher Scientific, Springfield, NJ). Coverslips were sterilized by rinsing in ethanol and allowed to dry under a sterile hood before they were immersed in a sterile fibronectin solution (25 μg/ml; Sigma) in Ca^{2+}- and Mg^{2+}-free Dulbecco's phosphate buffered saline (DPBS; Sigma) for 16 h at 4°C. Coverslips were then rinsed with sterile DPBS and used immediately for cell culture.

Cell Culture

The rat aortic smooth muscle cells (SMCs; line A10, American Type Culture Collection, Manassas, VA) were routinely maintained in Medium 199 (Gibco Invitrogen, Carlsbad, CA) supplemented with 10% heat-inactivated fetal bovine serum (Gibco), 100 U/ml of penicillin G sodium, 100 μg/ml of streptomycin sulfate, and 0.25 μg/ml of amphotericin B (Fungazone, Gibco). For staining experiments, subconfluent cultures were rinsed with DPBS, and cells were detached from culture dishes with 0.05% trypsin/ethylene-diamine-tetraacetic acid (Sigma). Care was taken to minimize cell clumping. Cells were seeded in culture medium on fibronectin-treated coverslips in eight-well polystyrene plates (Nalgene, Nunc, Rochester, NY) at a density of approximately 2,000/cm^2 and incubated for 24 h at 37°C and 5% CO_2.

Preparation of Labeling Solutions

N′N-dimethylformamide (DMF), dimethyl sulfoxide (DMSO), and FITC were obtained from Aldrich (St. Louis, MO). Fluorescein-5-maleimide, 5-IAF, F-NHS, CMFDA (CellTracker green), and fluorescein-DHPE were purchased from Molecular Probes (Eugene, OR). Individual stock solutions were prepared by dissolving FITC, 5-IAF, F-NHS, and fluorescein-5-maleimide in DMF (10 mg/ml). For staining, FITC and 5-IAF stock solutions, diluted 100-fold with 10 mM Na_2CO_3, pH 9.5, were added to the fixed cells. The high pH buffer afforded better reactivity of the cell components with the dyes. For staining with fluorescein-5-maleimide and F-NHS, stock solutions were diluted 100-fold in DPBS and added to the fixed cells. We later used fluorescein-5-maleimide at a 1:3,000 dilution and obtained similar labeling results. Fluorescein-DHPE in CH_3Cl (1 mg/ml, 50 μL) was taken to dryness with a stream of N_2 and dissolved in DMF at 1 mg/ml. The fluorescein-DHPE staining solution was prepared by dilut-

ing the stock solution 100-fold with DPBS containing 0.1% Triton X-100 (Sigma). The addition of detergent reduced the presence of bright punctuate background fluorescence with little influence on the cell membrane staining intensity. CMFDA in DMSO was prepared as instructed by the manufacturer.

Preparation of Mowiol Mounting Solution

Mowiol 4-88 (1.0 g; Polysciences, Warrington, PA) was mixed with 0.1 M Tris, pH 8.5, containing 25% glycerol (10 ml). The solution was mixed at room temperature for 2 h and then at 50°C for 1 h. The suspension was centrifuged at 5,000*g* (15 min), and the supernatant was collected. Diazobicyclo-octane (0.25% w/v; Aldrich), a free-radical scavenger that reduces photobleaching, was added, and aliquots were frozen at −20°C until use. Mowiol mounting medium was warmed to room temperature before use.

Cell Labeling

After incubation of cells for 24 h on fibronectin-coated coverslips, the cell culture plates were removed from the incubator, and the medium was carefully aspirated from each well. Nonadherent cells were removed by tilting the plate at approximately 30 degrees and gently flowing DPBS (~1.5 mL) across the coverslip surface while simultaneously aspirating with a Pasteur pipet placed at the lower edge of the well. With the exception of the cells stained with CMFDA, samples were fixed for 30 min with 4% formaldehyde in DPBS at room temperature and permeabilized with 0.1% Triton X-100 for 5 min. Samples were rinsed with DPBS, and the staining solutions were added (60 min at room temperature). After the staining solutions were removed, the samples were rinsed three times with DPBS and mounted by inverting the coverslips onto glass slides with a drop of Mowiol mounting solution. Live cells were stained with CMFDA as instructed by the manufacturer (1 μM CMFDA concentration, 60-min incubation in serum-free Medium 199 at 37°C), fixed with 4% formaldehyde, and mounted with Mowiol.

Coverslips were carefully placed on the glass slides to minimize the formation of trapped air bubbles. We also attempted to place the coverslips flat on the microscope slide to ensure that cells would be in the same focal plane in each area on the coverslip. Mounted coverslips were allowed to harden at room temperature and stored at −20°C until use (typically 2 days). Some samples were kept for several months to determine how long-term storage influences the staining pattern.

Fluorescence Microscope and Image Processing

An inverted Axiovert S100 TV epifluorescence microscope (Carl Zeiss, Thornwood, NY), a CoolSNAP FX CCD camera (1,300 × 1,030 imaging pixels, 6.7- × 6.7-μm pixels, operated at −30°C; Roper Scientific/Photometrics, Tucson, AZ) and an X,Y translation stage (Ludl Electronic Products, Hawthorne, NY) were under computer control of the image processing software (Inovision, currently ISee; Imaging Systems, Raleigh, NC). The fluorescence excitation source was a variable-intensity 100-W AttoArc 2 mercury arc lamp (Atto Instruments, Rockville, MD). The fluorophore-labeled cells were visualized through a Chroma 41001 filter set (EX 480/40, EM 535/50, BS Q505lp) optimized for fluorescein. Images for automated analysis were collected with a 10×, 0.25 numerical aperture, Ph1 A-Plan objective (Carl Zeiss). A sampling and analysis routine was set up within the image processing software to systematically collect 110 images (~0.66 cm^2 total sampling area) and perform object detection and corresponding shape analysis of cells in each frame. Each frame from the CCD camera (325 × 257 pixels, 4 × 4 binning) consisted of an 870- × 690-μm area. For each frame, the stage was automatically moved 1,000 μm in the x direction or 800 μm in the y direction, thus allowing distances longer than 100 μm between frames. This eliminated the chance of counting the same cells more than once.

Each image was treated with a series of image processing algorithm modules as it was collected. The first module (Features) identifies objects based on a threshold value and size criterion, as discussed below. The Features module presents each object detected to the Shape module. The Shape module determines the physical properties of the object's shape. Among these properties are area, perimeter, axial ratio, and roundness. The objects detected in the Features module are also directed to a Histogram module to determine the average pixel intensity of each object. Values for each object were saved in text files that were analyzed with a spreadsheet program.

Exposure times were determined empirically for each treatment by comparing the ratio of pixel intensities within the cell areas with the intensities in non-cell areas (e.g., background). The minimum exposure time above which this ratio did not significantly change was used for image collection. The exposure times were approximately 0.03–1 s when the camera was set to 4 × 4 binning and the excitation lamp intensity was at 30% of its full output. Threshold values for cell edge detection initially were chosen as a value approximately 100 units above the average background value. This threshold value was then tested by examining several frames and confirming that cells were accurately identified and background areas were not detected as cell areas. In some cases, coverslips were analyzed with several different threshold values to examine the effect of threshold value on detected cell area. Cells also were discriminated by pixel area. The limiting area values were determined empirically by evaluating the area of small and large bright objects. Only objects with areas between 50 and 5,000 pixels were considered to be cells and included in the analysis. Background levels were determined by manually examining several frames and determining the average pixel intensity values at random non-cell areas. It is important to note that the microscope lamp focus was adjusted to minimize illumination variations across the collected CCD image.

A sample was mounted in the translation stage, the first field was brought into focus, and the scanning routine was initiated. The collection times for frames in each 22- ×

22-mm coverslip were briefer than 5 min. Image collection and automated object detection were monitored during program execution; when object detection difficulties were observed, the program was stopped and threshold values were adjusted. The program was then initiated from the beginning.

SDS-PAGE Analysis of Cells Stained With Fluorescein-5-Maleimide

SMCs were cultured in a 100-mm Petri dish, fixed, and stained with fluorescein-5-maleimide, as described above. Cells were lysed in 1× SDS polyacrylamide gel electrophoresis (PAGE) sample buffer (300 μL; Bio-Rad, Hercules, CA), and proteins were separated on a 12% SDS-PAGE gel (31). Fluorescent proteins were visualized on an ultraviolet transillumination tray equipped with a CCD camera (Alpha Innotech, San Leandro, CA). Molecular weights were determined with prestained protein standards (Bio-Rad).

RESULTS

Selection of Fluorescent Dyes

We compared several fluorescent dyes for their relative efficiency in automated determination of cell shape and area. Accurate assessment of cell area and shape requires accurate assignment of the cell perimeter and the ability to unambiguously distinguish the cell at its perimeter from the non-cell background. Figure 1 shows phase-contrast (Fig. 1A) and fluorescent micrographs of SMCs after treatment with the indicated dyes. The contrast and brightness of the fluorescent pictures were adjusted to optimize visualization of the staining pattern over the entire area of the cell. This method saturates intensity values (white color) in some areas of the cells.

A fixed SMC stained with CMFDA is shown in Figure 1B. This is a thiol-reactive non-fluorescent vital stain that becomes fluorescent when the acetate groups are removed via esterases within a living cell (32). This reagent labels sulfhydryl-containing proteins and other biomolecules in the cytoplasmic space and provides identification of the cell perimeter. We also stained fixed SMCs with other fluorescent compounds that become covalently coupled to functional groups within proteins. Figures 1C–F show cells stained with fluorescein-5-maleimide, 5-IAF, F-NHS, and FITC, respectively. The iodoacetamide and maleimide groups react primarily with free sulfhydryl groups (33). F-NHS and FITC react with primary amino groups on proteins or lipids (33). The images indicated that each compound is capable of labeling cellular components, thereby allowing identification of the cell perimeter. Cells treated with these dyes showed brightest staining in the nuclear region of the cell (Fig. 1C–F), likely due to the greater thickness of the cell in the nuclear region. The fine structure of the cytoskeleton was best observed in cells labeled with the fluorescein-5-maleimide conjugating reagent (Figs. 1C and 5), suggesting the reagent reacts with intracellular cytoskeletal proteins.

Figure 1G shows fixed SMC stained with fluorescein-DHPC. This fluorescent molecule is a phospholipid and is presumed to associate primarily with the cellular membrane. The cell membrane appeared homogeneously labeled, and stained cytoskeletal structures were not observed. Although the staining in the central parts of the nucleus was reduced compared with the surrounding area, the contrast enhancement used to show the cell perimeter in Figure 1G resulted in saturation of the pixels in the center of the cell.

Quantitative Microscopy

Table 1 compares quantitative data for the different dyes. Different exposure times were used for each dye. These times were identified as exposure times above which the ratio of the average cell intensity over the average background intensity did not significantly change (i.e., the maximum signal-to-noise ratio was achieved). Identification of the minimal exposure time that achieves the best signal-to-noise ratio maximizes the data collection efficiency and minimizes photobleaching. Typically, the brightest areas of the stained cells saturate up to 1% of the CCD camera pixels at the exposure time required for maximal contrast.

Cells stained with CMFDA, fluorescein-5-maleimide, FITC, 5-IAF, and F-NHS had similar average cell signal intensities, but the exposure times for achieving maximal contrast ranged from 0.03 s for fluorescein-5-maleimide to 1.0 s for CMFDA. The variation in average cellular intensity between replicate coverslips was less than 9% for these stains (Table 1). The fluorescein-DHPE–stained cells exhibited the highest average cell intensity due to more homogeneous staining across the cell surface (~37% intensity variation over the cell) when compared with cells stained with the other dyes (~70% intensity variation over the cell). Despite the higher average cell intensity, an exposure time of 0.7 s was required to achieve maximal contrast of cells stained with the fluorescent lipid because of the high level of background fluorescence.

Background levels were determined by randomly evaluating pixel intensities at non-cell areas in several different areas of the coverslips. Variations in background levels were less than 5% across an approximately 1-cm^2 area of the coverslip (data not shown). In all cases, average variation in background levels between replicate coverslips treated with the chemically reactive dyes was less than 23% of the average (Table 1). The background levels resulting from the chemically reactive dyes were of interest because the surfaces were coated with fibronectin, a protein with free sulfhydryl and amino groups. For the exposure times that were used, the background signals for the chemically reactive dyes were not significantly different from those observed from CMFDA, a vital stain that requires cytoplasmic esterase activity to activate fluorescence (Table 1). This result indicated that signal due to adsorption or conjugation of the chemically reactive dyes to the matrix proteins is not necessarily a significant problem. The cell samples labeled with fluorescein-DHPE exhibited the highest background intensity, likely due to nonspecific adsorption of the hydrophobic lipid to the substrate surfaces.

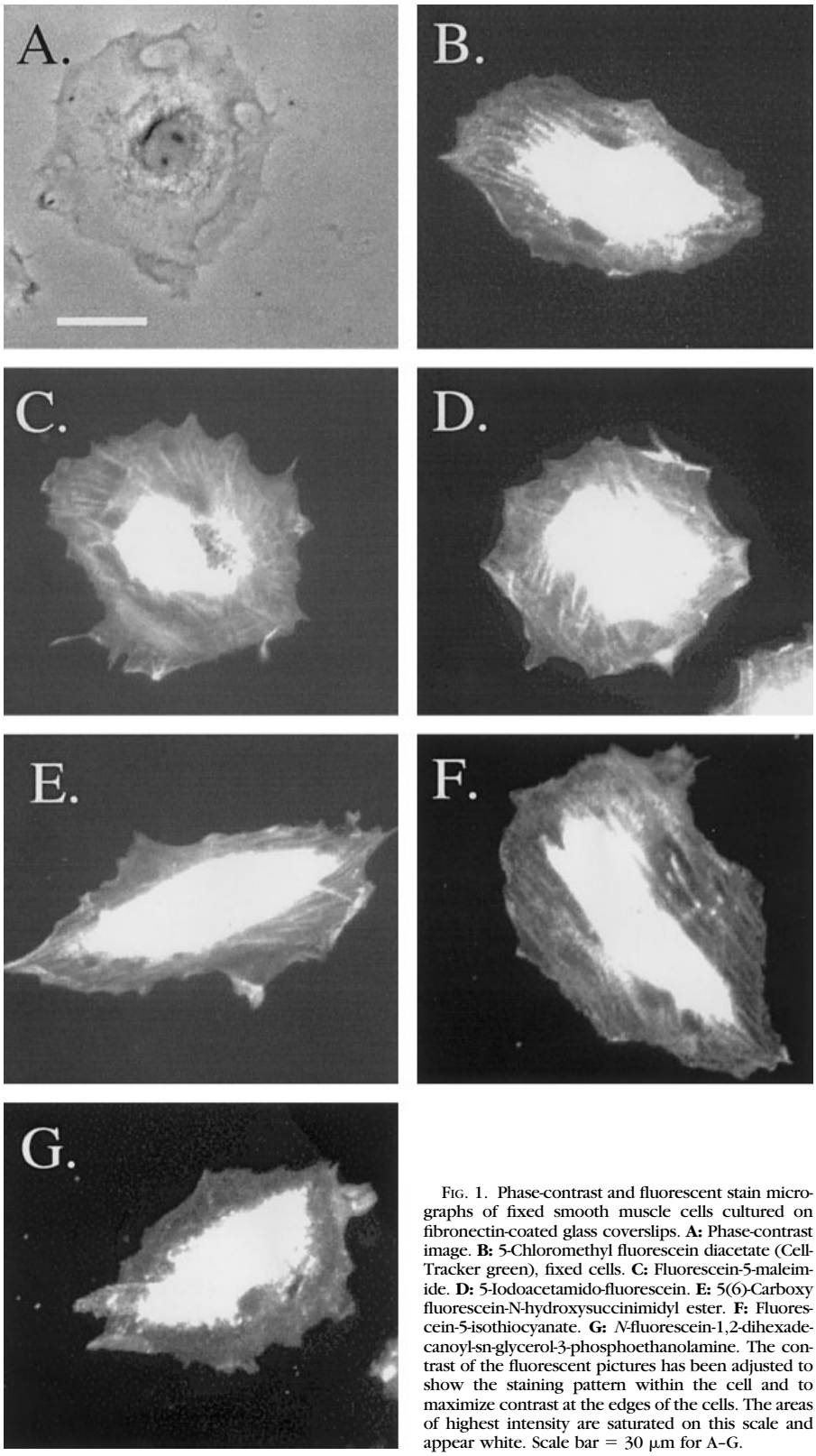

FIG. 1. Phase-contrast and fluorescent stain micrographs of fixed smooth muscle cells cultured on fibronectin-coated glass coverslips. **A:** Phase-contrast image. **B:** 5-Chloromethyl fluorescein diacetate (CellTracker green), fixed cells. **C:** Fluorescein-5-maleimide. **D:** 5-Iodoacetamido-fluorescein. **E:** 5(6)-Carboxy fluorescein-N-hydroxysuccinimidyl ester. **F:** Fluorescein-5-isothiocyanate. **G:** *N*-fluorescein-1,2-dihexadecanoyl-sn-glycerol-3-phosphoethanolamine. The contrast of the fluorescent pictures has been adjusted to show the staining pattern within the cell and to maximize contrast at the edges of the cells. The areas of highest intensity are saturated on this scale and appear white. Scale bar = 30 μm for A–G.

Table 1
Experimental Values From Automated Microscopy Analysis of Fixed Cells Stained With Fluorescent Reagents

Fluorescent reagent[f]	Exposure[b] time/frame (s)	Average background intensity[c,d]	Average cell intensity[c]	Threshold[e]
CMFDA[a], fixed cells	1	300 ± 12	1,228 ± 6	≈400
Fluorescein-5-maleimide	0.03	129 ± 3	1,345 ± 32	≈230
FITC	0.04	195 ± 8	1,417 ± 74	≈300
5-IAF	0.07	144 ± 6	1,332 ± 53	≈250
F-NHS	0.05	312 ± 71	1,476 ± 110	≈410
Fluorescein-DHPE	0.7	722 ± 192	2,274 ± 219	≈820

[a]Cells were stained before fixing.
[b]Lamp intensity at 30%, CCD camera set to 4 × 4-pixel binning.
[c]Average standard deviation from three coverslips.
[d]Background variation across a 1-cm^2 area of each coverslip was less than 5%.
[e]Threshold used to determine the average cell intensity was set to ≈100 units above the average background of each coverslip.
[f]5-IAF, 5-iodoacetamidofluorescein; CMFDA, 5-chloromethyl fluorescein diacetate: FITC, fluorescein-5-isothiocyanate; fluorescein-DHPE, *N*-fluorescein-1.2-dihexadecanoyl-sn-glycerol-3-phosphoethanolamine; F-NHS, 5(6)-carboxy fluorescein-N-hydroxysuccinimidyl ester.

Thresholding and Quantitative Analysis

The average fluorescence intensity was determined for a statistically large number of cells by using automated microscopy. Before automated data collection, threshold values and size limits to be used for object detection were determined as described in Materials and Methods. In general, the threshold values were approximately 100 units above the background signal (Table 1). These values allowed accurate cell detection but eliminated identification of non-cell areas that exhibited high background levels.

When using the appropriate thresholding and size criteria, digital image analysis yielded the average signal intensity within each object detected. Between approximately 800 and 1,100 objects were detected in 110 frames; thus a mean intensity per cell and a corresponding population distribution of intensities were determined. The mean intensity values for the SMCs treated with the various fluorophores are shown in Table 1. A summary of the fluorescence intensity data for all of the reagents and the staining procedures used in this study are shown in Figure 2. These data are presented as a ratio of average intensity to background intensity for the exposure times shown in Table 1. The fluorescein-5-maleimide–labeled cells have an average intensity that is approximately threefold greater than CMFDA with a 30-fold lower exposure time. Although the standard deviation in average cell intensity between replicate coverslips was small (<9%, Table 1), the standard deviation bars shown in Figure 2 represent the width of the distribution of fluorescence intensities between cells in the population. Thus, 67% of all the cells examined had fluorescence intensities within these bars.

Figure 2 (inset) also shows the ratio of average cell to background intensities for each fluorescent reagent after normalizing for exposure time. The time-normalized signal-to-background ratio of the fluorescein-5-maleimide–labeled cells was approximately 100-fold larger than that for CMFDA. This difference was due to the greater fluorescence intensity ratio and the shorter exposure time required to achieve maximal contrast with the fluorescein-5-maleimide probe. We found that cells stained with each of the chemically reactive fluorophores were significantly brighter than the cells stained with CMFDA when using procedure described in Materials and Methods. The exposure time-normalized signal-to-noise ratio for the fluorescein-DHPE–labeled cells was similar to that for the CMFDA-labeled cells.

Apparent Cell Area Determination

In general, for all dyes studied, the staining intensity was strongest near the nucleus and weakest at the cell edge (Fig. 1). This demonstrated the challenge to accurate cell size and shape analysis: the fluorescent label must provide sufficient contrast at the cell perimeter where the effective pathlength is short. To identify which label provided the best discrimination of the cell edge, we compared the average area per cell object for cells treated with the different fluorophores. In addition, the average area was determined at multiple threshold values for some of the stains to probe the sensitivity of threshold choice to the accurate determination of the cell periphery. These data are shown in Figure 3.

The average area of the SMCs cultured on fibronectin-coated coverslips was first determined by manually outlining more than 140 fixed cells and introducing these objects into the Shape module in the image processing software. Labeled cells on identically prepared coverslips were then evaluated by the automated routine, where the areas of approximately 800 cells were averaged. Figure 3 shows that, at the lowest suitable threshold value (50 or 100 intensity units above background), the average area of the cells labeled with each of these dyes was approximately equal to that determined manually. This observation indicated that each label evaluated in this study and the methodology used to determine the selection criteria can be used to accurately determine the cell area of fixed cells.

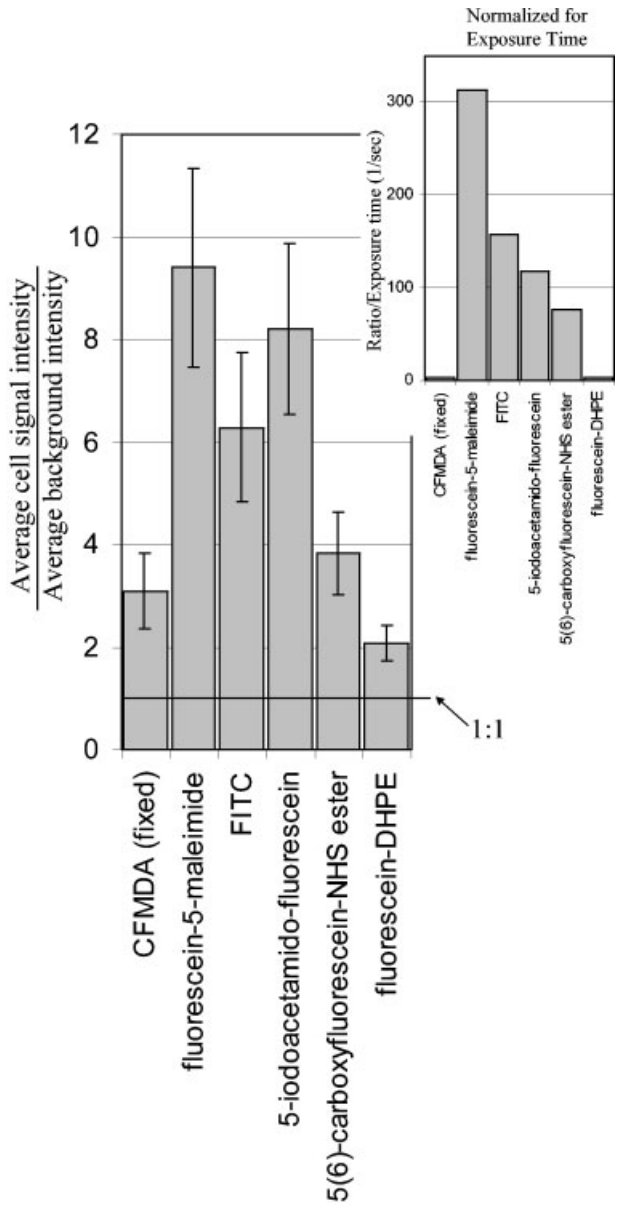

FIG. 2. Average signal-to-noise ratio for fluorescently stained cells. The average signal intensity of cells detected in 110 images was divided by the average background signal in the area between cells. The error bars represent the standard deviation of this distribution from the mean intensity and indicate that the population consists of cells with variable fluorescent intensities. Approximately 67% of the cells detected had average intensities within these error bars. The signal-to-noise ratios and standard deviation error bars are an average from three coverslips. When the signal-to-noise ratio was normalized for exposure time (inset), fluorescein-5-maleimide–labeled cells were determined to be approximately 100-fold brighter than the CMFDA-labeled cells. CMFDA, 5-chloromethyl fluorescein diacetate; FITC, fluorescein-5-isothiocyanate; fluorescein-DHPE, *N*-fluorescein-1,2-dihexadecanoyl-sn-glycerol-3-phosphoethanolamine.

CMFDA-, FITC-, and fluorescein-5-maleimide–labeled cells were then evaluated at threshold values that were raised in 50-unit increments up to 200 intensity units above background. At the highest threshold value examined, only the cell area determined from the CMFDA-labeled cells was significantly less than that determined manually (Fig. 3). An identical number of objects was detected at each threshold setting for the respective dyes, indicating that the decrease in area was due to a change in the detected cell perimeter and not to a failure of recognizing cells as counted objects. These data indicated that the fluorescein-5-maleimide and FITC stains are less sensitive to the chosen threshold value when compared with cells stained with CMFDA.

The effect of the threshold value on apparent cell area is shown in Figure 4. Using a low threshold value only 5 intensity units above the average background levels for CMFDA-treated cells provided excellent edge detection of the well-spread cell shown in the lower left area of Figure 4A. However, this same threshold value also resulted in counting some of the background area in the upper right corner of the frame incorrectly as corresponding to cell fluorescence. Raising the threshold by 40 intensity units allowed the appropriate edge detection of the three cells in the upper right area of the frame, but it identified only the center of the well-spread cell in the lower left corner, resulting in a decrease in the apparent average cell area. Edge detection of the fluorescein-5-maleimide–labeled cells is shown in Figure 4C. At a lower threshold value, correct perimeter detection of the well-spread cells on the left and right occurred. This threshold value was 100 units above the average background value. When the threshold value was increased by 80 intensity units, the edge of the cell on the right was correctly identified, but there is a decrease in the detected area of the cell on the left. These effects are reflected in the average area values shown in Figure 3.

Proteins Labeled With Fluorescein-5-Maleimide

To our knowledge, fluorescein-5-maleimide, the brightest cell label identified in this study, has not been used previously as a cell stain. Figure 5A shows a fluorescent micrograph of the fixed SMCs labeled with fluorescein-5-maleimide. The contrast and brightness of the image were adjusted to visualize the labeling pattern. Maleimides nonspecifically react with free sulfhydryl groups on cysteine side chains. The cytoskeletal labeling pattern indicated that the fluorescein-5-maleimide passes across the cell membrane and reacts with several cytoskeletal proteins. Further, the reagent likely labeled other cytoplasmic proteins with free sulfhydryl groups. We analyzed the labeled proteins by SDS-PAGE gels (Fig. 5B). Proteins at molecular weights of 25, 35, 37, 55, and approximately 125 kDa were clearly visible when the gel was visualized under ultraviolet light. We do not know whether these proteins were specific cytoskeletal proteins. A fluorescent signal also was observed throughout the separated proteins, but it was unclear what fraction of this signal was due to proteins that were cross-linked due to formaldehyde fixation.

DISCUSSION

Quantitative evaluation of cell morphology can be performed manually on a limited number of images, but

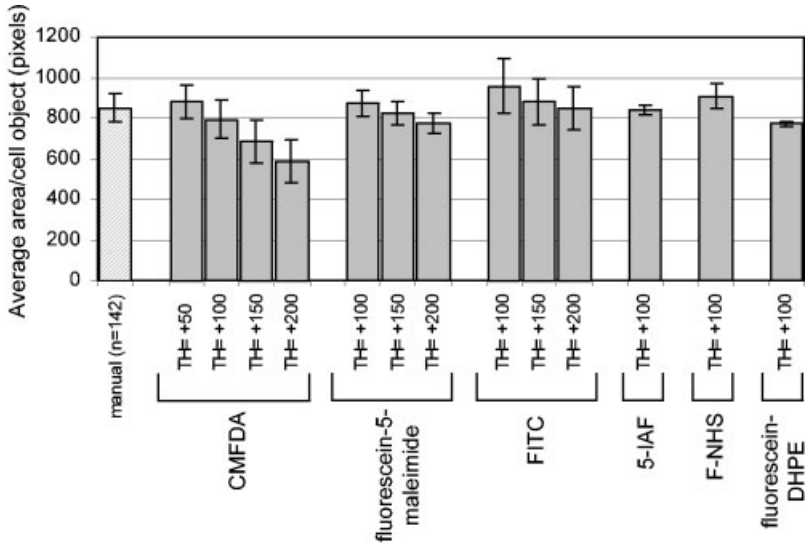

FIG. 3. Apparent average cell area determined with different threshold values. Quantitative microscopy was used to determine the average cell area from fixed cells labeled with CMFDA, fluorescein-5-maleimide, FITC, F-NHS, 5-IAF, and fluorescein-DHPE. Coverslips for each stain were prepared in an identical fashion. An average area for 142 non-labeled cells on a coverslip was calculated by manually outlining the cell objects (error bars = standard deviations, where n = 3 sets of frames). By using automated sampling and analysis, the average cell area was determined at threshold values (TH) 50 (CMFDA) or 100 intensity units above background. Average cell area for cells stained with CMFDA, fluorescein-5-maleimide, and FITC also were determined at higher TH values. Exposure times and average background fluorescence for the treated cells are shown in Table 1. Error bars represent the standard deviation from three coverslips. 5-IAF, 5-iodoacetamidofluorescein; CMFDA, 5-chloromethyl fluorescein diacetate; FITC, fluorescein-5-isothiocyanate; fluorescein-DHPE, *N*-fluorescein-1,2-dihexadecanoyl-sn-glycerol-3-phosphoethanolamine; F-NHS, 5(6)-carboxy fluorescein-N-hydroxysuccinimidyl ester.

automated image processing software coupled to automated stage movement and field selection can be used to improve sampling and data collection efficiency by allowing a statistically significant number of cells to be quantified. Optical discrimination of the cell edge above a non-cell background is essential for accurate determination of cell morphology. In this study, we examined several fluorescent reagents and evaluated their use as stains for morphologic analysis of fixed cells with the use of automated procedures. We identified a fluorescent reagent, fluorescein-5-maleimide, that is approximately 100-fold more intense (Fig. 2, inset) than the cytoplasmic CMFDA vital stain and confers excellent contrast at the cell periphery. Sufficient contrast for cells labeled with fluorescein-5-maleimide could be achieved with exposure times of 0.03 s by using the experimental setup described in Materials and Methods. This fluorophore can be used after the cells have been fixed with formaldehyde, a feature that may facilitate high -throughput protocols, and the stained cells showed little loss in signal intensity even after the slides had been stored for several months. Our study also found that several chemically reactive fluorescein-based reagents are suitable stains for rapid automated morphologic analysis of fixed cells. Cells stained with FITC, 5-IAF, and F-NHS were significantly brighter than the CMFDA-labeled cells.

Our studies were initiated because traditional non-fluorescent cytoplasmic stains (e.g., toluidine blue O, Coomassie blue) failed to provide sufficient contrast near the edge of well-spread cells. We then used CMFDA, a membrane-permeable, thiol-reactive fluorescein derivative that requires intracellular esterase activity to generate the fluorescent molecule. Sufficient edge contrast to determine accurate cell areas by automated methods was possible with this dye when exposure times on the order of 1 s were used. Although this exposure time was reasonable for the experiments that were performed in this study, we deemed it was too long for applications that require the collection of multiple images (e.g., auto-focusing) or for analysis of larger numbers of fields (e.g., when examining larger numbers of samples or larger coverslips). In these studies, CMFDA was used at a 1 μM concentration as recommended, although the manufacturer indicated that higher concentrations of CMFDA can be used.

We hypothesized that fluorescent reagents that concentrate the fluorescent groups at the edge of the cell would provide good contrast at the cell periphery. Labeling with a fluorescent phospholipid did highlight the cell edge, but the low level of fluorescence staining and the high background levels (Figs. 1G and 2) resulted in the need to use long exposure times to attain maximal contrast. We then attempted to use fluorescent reagents that are commonly used to modify amino- (lysine and N-terminal) and sulfhydryl- (cysteine) containing side chains on proteins. NHS esters and isothiocyanates covalently react with amino groups. Cells stained with FITC and F-NHS resulted in bright cells with high contrast at the cell periphery (Figs. 1 and 2). FITC has been used to fluorescently label live cells (34), but it is not routinely used to label fixed cells. Cell periphery staining also was observed with fluorescent reagents that interact with sulfhydryl groups. The results from the cells labeled with 5-IAF were similar to those obtained with amino reactive reagents (Fig. 2). Cells stained with fluorescein-5-maleimide exhibited the highest exposure time-normalized signal-to-noise ratio (Fig. 2, inset) compared with the other dyes used in this study. The maleimide group is highly reactive with free thiols at pH.7.5 (33). The CMFDA reagent also reacts with thiol groups in biomolecules, but the staining intensity was significantly less than with the other thiol-reactive probes used in this study. We expect that the difference in stain intensity was due to the lower concentration of CMFDA used to label the live cells or to a low level of esterase activity in the thin periphery regions of the well-spread SMCs. It is worth noting that the Mowiol mounting me-

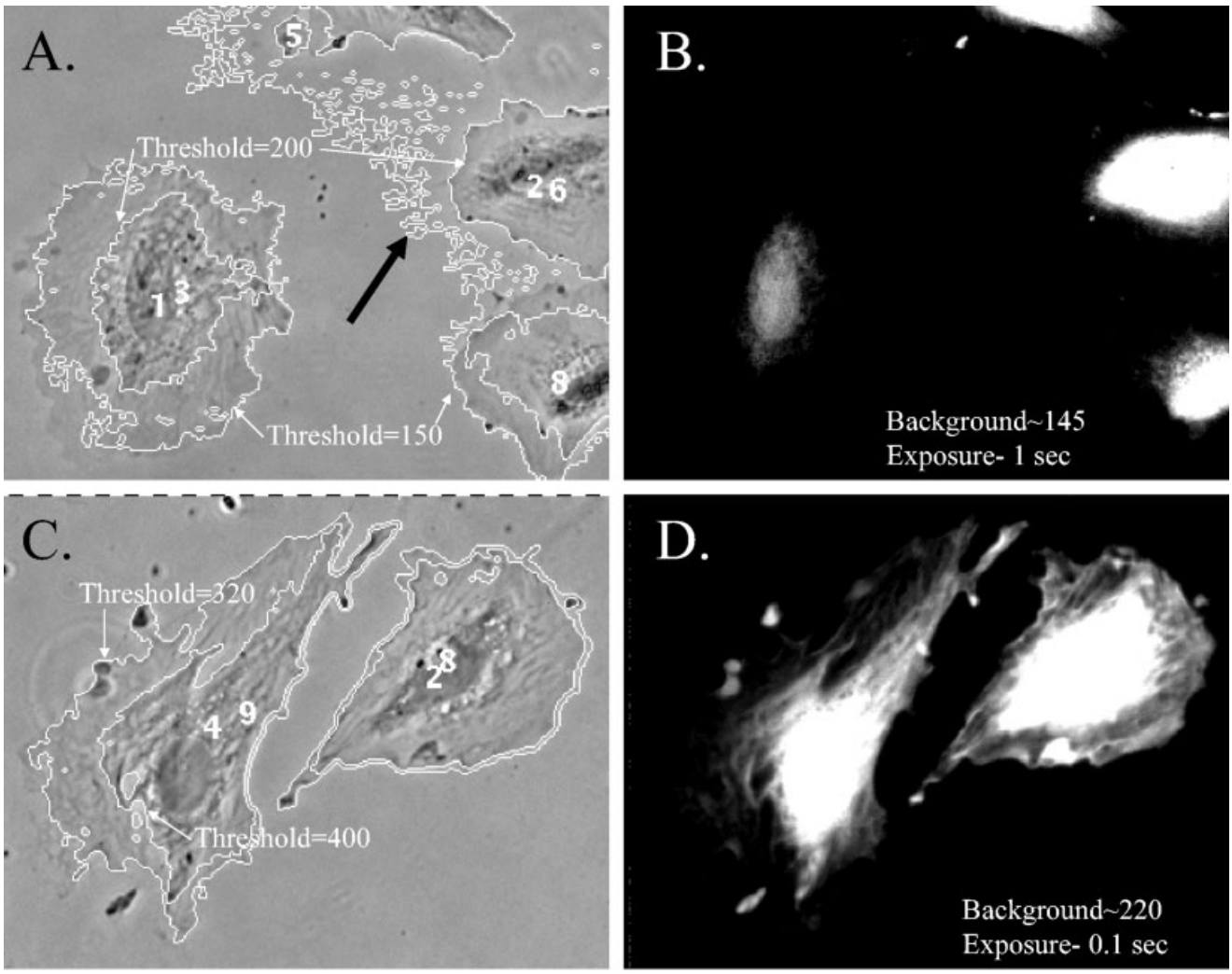

FIG. 4. Changes in detected cell areas at two different thresholds. Phase-contrast (**A, C**) and corresponding fluorescent (**B, D**) images of cells labeled with CMFDA (A, B) and fluorescein-5-maleimide (C, D) are shown. The edge of a well-spread cell stained with CMFDA could be detected with a threshold 5 units above background (A), but this threshold value also caused nonspecific detection of background areas (arrow). Raising the threshold value 40 units resulted in edge detection of the three cells in the right side of the panel, but the only the central area of the well-spread cell was detected. Edges of the fluorescein-5-maleimide–labeled cells were correctly detected with a threshold value 100 units above the average background (C). Raising the threshold value 80 units resulted in reduced area detection of the well-spread cell on the left. Edge detection is less sensitive to threshold adjustments with the fluorescein-5-maleimide–stained cells. Fluorescent images are contrast enhanced to the same scale to compare intensity differences. CMFDA, 5-chloromethyl fluorescein diacetate.

dium was at pH 8.1, which is nearly optimal for maximum fluorescein emission (35).

Although the covalent coupling dyes may label the extracellular matrix proteins present on the cell culture substrates and the cellular proteins leading to a decrease in signal-to-background ratio, this was not a problem with the reagents used in this study because the fluorescence of cells was so much higher than the background signal. However, with sufficient exposure times, it was apparent that the fibronectin on the glass coverslips was labeled. Thus, the use of chemically reactive fluorescent reagents may be problematic if they are used to image cells cultured on materials containing the reactive functional groups or gel materials that retain the staining solution. An advantage of using CMFDA is that it requires intracellular esterase activity to become fluorescent and has minimal fluorescence outside a cell (32).

Fluorescein-5-maleimide was the brightest cell-labeling agent identified in this study. Upon further inspection of the fluorescein-5-maleimide–labeled cells, the cytoskeletal proteins appeared to be labeled with the fluorophore (Fig. 5). This observation suggested that formaldehyde fixation does not inactivate the free thiol groups on the cellular proteins. One of the advantages of using maleimide-based reagents for cell labeling is the variety of fluorescent maleimide compounds with different spectral properties that are available. Our preliminary results with Texas Red C2 maleimide and Cy5 maleimide (36) in fixed cells were

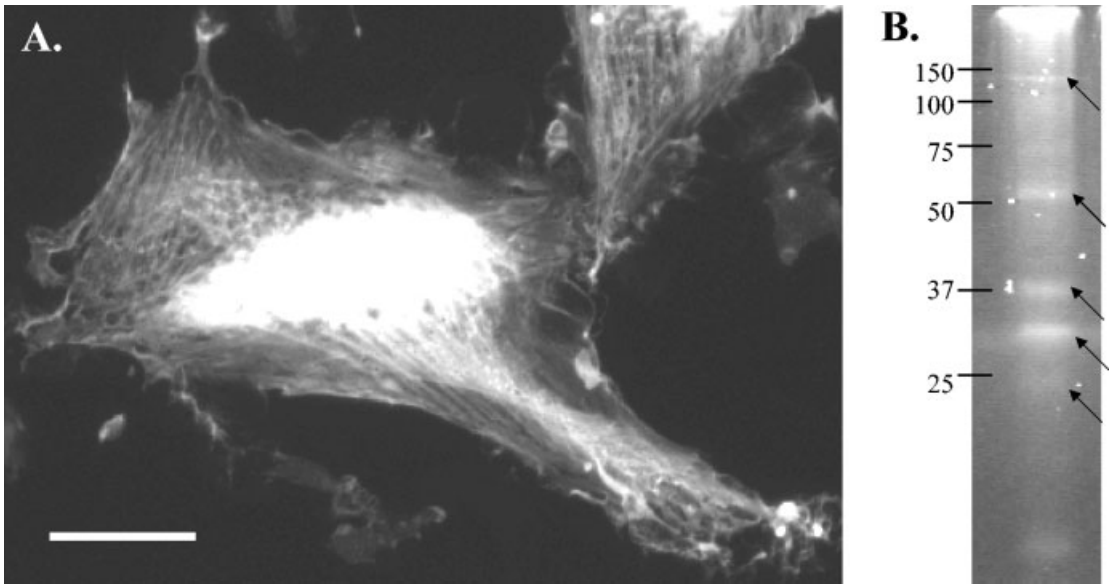

FIG. 5. Analysis of fluorescein-5-maleimide–labeled proteins. Rat smooth muscle cells were cultured on tissue-culture polystyrene, fixed, permeabilized with 0.1% Triton X-100, and stained with fluorescein-5-maleimide. **A:** Fluorescent micrograph of labeled cells. Cytoskeletal-like fine structures can be observed within the cell. Scale bar = 20 μm. **B:** The cell proteins were separated by 12% sodium dodecyl sulfate polyacrylamide gel electrophoresis (SDS-PAGE) and visualized under ultraviolet light. Labeled proteins at molecular weights of 25, 35, 37, 55, and approximately 125 kDa can be observed in the SDS-PAGE gel.

very successful. SDS-PAGE analysis and fluorescent micrographs indicated that the cell components that are labeled appear to be identical to those labeled by fluorescein-5-maleimide. The results suggested that other fluorescent maleimides may be useful for cellular staining and applications that require automated cell edge detection.

In this study, the cell density on the coverslips was purposely kept low (~2,000 cells/cm^2) to minimize the occurrence of groups of cells in which individual cells cannot be easily distinguished when using automated image processing. By visually examining images, we estimated that, even at this density, up to 20% of the "objects" detected by the automated methods were composed of two or more cells. This resulted in the average reported cell area being approximately 10% larger than that for individual cells. For samples in which cells are denser and more often clustered, we propose using a nuclear stain in conjunction with a cell edge stain to identify the total number of nuclei in any detected cell area (36). Such a procedure permits accurate determination of average cell area of individual cells and groups of cells.

LITERATURE CITED

1. Fung DC, Theriot JA. Imaging techniques in microbiology. Curr Opin Microbiol 1998;1:346–351.
2. Jonker A, Geerts WJ, Chieco P, Moorman AF, Lamers WH, Van Noorden CJ. Basic strategies for valid cytometry using image analysis. Histochem J 1997;29:347–364.
3. Goldstein E, Donovan RM, Kim Y. Applications of computerized microscopic image analysis in infectious diseases. Rev Infect Dis 1988;10:92–102.
4. Kiernan JA. Histological and histochemical methods: theory and practice. Oxford: Butterworth-Heinemann; 2000.
5. Wouters FS, Verveer PJ, Bastiaens PI. Imaging biochemistry inside cells. Trends Cell Biol 2001;11:203–211.
6. Johnson I. Fluorescent probes for living cells. Histochem J 1998;30: 123–140.
7. Wittekind D. Standardization of dyes and stains for automated cell pattern recognition. Anal Quant Cytol 1985;7:6–30.
8. Cunningham RE. Overview of flow cytometry and fluorescent probes for cytometry. Methods Mol Biol 1994;34:219–224.
9. Haugland RP. Handbook of fluorescent probes and research chemicals. Eugene, OR: Molecular Probes; 1996.
10. Paddock SW. Imaging techniques: picture the world with kaleidoscope dyes. Curr Biol 1997;7:R182–R185.
11. Mehes G, Lorch T, Ambros PF. Quantitative analysis of disseminated tumor cells in the bone marrow by automated fluorescence image analysis. Cytometry 2000;42:357–362.
12. Oosterwijk JC, Knepfle CF, Mesker WE, Vrolijk H, Sloos WC, Pattenier H, Ravkin I, van Ommen GJ, Kanhai HH, Tanke HJ. Strategies for rare-event detection: an approach for automated fetal cell detection in maternal blood. Am J Hum Genet 1998;63:1783–1792.
13. Mesker WE, vd Burg JM, Oud PS, Knepfle CF, Ouwerkerk-v Velzen MC, Schipper NW, Tanke HJ. Detection of immunocytochemically stained rare events using image analysis. Cytometry 1994;17:209–215.
14. Tanke HJ, Oosterwijk JC, Mesker WE, Ouwerkerk van-Velzen MC, Knepfle CF, Wiesmeyer CC, van Ommen GJ, Kanhai HH, Vrolijk J. Detection of 'rare event' fetal erythroblasts in maternal blood using automated microscopy. Early Hum Dev 1996;47:S89–S93.
15. Ploem JS, van Driel-Kulker AM, Goyarts-Veldstra L, Ploem-Zaaijer JJ, Verwoerd NP, van der Zwan M. Image analysis combined with quantitative cytochemistry. Results and instrumental developments for cancer diagnosis. Histochemistry 1986;84:549–555.
16. Kraeft SK, Sutherland R, Gravelin L, Hu GH, Ferland LH, Richardson P, Elias A, Chen LB. Detection and analysis of cancer cells in blood and bone marrow using a rare event imaging system. Clin Cancer Res 2000;6:434–442.
17. van Raaij EJ, ten Berge D, Hage W, Brouwer A, Meijlink F, Maintz JB, Verbeek FJ. Automated topographical cell proliferation analysis. Cytometry 2001;45:13–18.
18. Darzynkiewicz Z, Bedner E, Li X, Gorczyca W, Melamed MR. Laser-scanning cytometry: a new instrumentation with many applications. Exp Cell Res 1999;249:1–12.
19. Zurgil N, Kaufman M, Solodiev I, Deutsch M. Determination of cellular thiol levels in individual viable lymphocytes by means of fluorescence intensity and polarization. J Immunol Methods 1999;229: 23–34.

20. Deutsch M, Kaufman M, Shapiro H, Zrgil N. Analysis of enzyme kinetics in individual living cells utilizing fluorescence intensity and polarization measurements. Cytometry 2000;39:36–44.
21. Bedner E, Melamed MR, Darzynkiewicz Z. Enzyme kinetic reactions and fluorochrome uptake rates measured in individual cells by laser scanning cytometry. Cytometry 1998;33:1–9.
22. Sunray M, Zurgil N, Shafran Y, Deutsch M. Determination of individual cell Michaelis-Menten constants. Cytometry 2002;47:8–16.
23. Chicurel ME, Chen CS, Ingber DE. Cellular control lies in the balance of forces. Curr Opin Cell Biol 1998;10:232–239.
24. Ingber DE. Tensegrity: the architectural basis of cellular mechanotransduction. Annu Rev Physiol 1997;59:575–599.
25. Dike LE, Chen CS, Mrksich M, Tien J, Whitesides GM, Ingber DE. Geometric control of switching between growth, apoptosis, and differentiation during angiogenesis using micropatterned substrates. In Vitro Cell Dev Biol Anim 1999;35:441–448.
26. Chen CS, Mrksich M, Huang S, Whitesides GM, Ingber DE. Geometric control of cell life and death. Science 1997;276:1425–1428.
27. Porter KR. Changes in cell topography associated with transformation to malignancy. Adv Pathobiol 1975;1:29–47.
28. Levine TS, Njemenze V, Cowpe JG, Coleman DV. The use of the PAPNET automated cytological screening system for the diagnosis of oral squamous carcinoma. Cytopathology 1998;9:398–405.
29. Bartels PH, Wied GL. Automated image analysis in clinical pathology. Am J Clin Pathol 1981;75:489–493.
30. Pakalns T, Haverstick KL, Fields GB, McCarthy JB, Mooradian DL, Tirrell M. Cellular recognition of synthetic peptide amphiphiles in self-assembled monolayer films. Biomaterials 1999;20:2265–2279.
31. Laemmli UK. Cleavage of structural proteins during the assembly of the head of bacteriophage T4. Nature 1970;227:680–688.
32. Poot M, Kavanagh TJ, Kang HC, Haugland RP, Rabinovitch PS. Flow cytometric analysis of cell cycle–dependent changes in cell thiol level by combining a new laser dye with Hoechst 33342. Cytometry 1991;12:184–187.
33. Hermanson GT. Bioconjugate techniques. San Diego: Academic Press; 1996.
34. Abernethy NJ, Chin W, Lyons H, Hay JB. A dual laser analysis of the migration of XRITC-labeled, FITC-labeled, and double-labeled lymphocytes in sheep. Cytometry 1985;6:407–413.
35. Sjoback R, Nygren J, Kubista M. Absorption and fluorescence properties of fluorescein. Spectrochim Acta A 1995;51:L7–L21.
36. Elliott JT, Woodward JT, Tona A, Jones PL, Plant AL. Thin films of collagen affect smooth muscle cell morphology. Langmuir 2002. Published Online, DOI 10.1021/la025609n.